The effect of scatter correction on planar and tomographic semiquantitative ^{123}I cardiac imaging. A phantom study

Emmanouil Papanastasiou[1] MSc, PhD
Efstratios Moralidis[2] MD, PhD
Anastasios Siountas[1] MSc, PhD

1. Department of Medical Physics, AHEPA University Hospital, Aristotle University Medical School, Thessaloniki Greece
2. Department of Nuclear Medicine, Papageorgiou General Hospital, Aristotle University Medical School, Thessaloniki Greece

Keywords: Scatter correction, -^{123}I cardiac imaging -Semiquantitative ^{123}I cardiac imaging

Corresponding author:
Emmanouil Papanastasiou, Department of Medical Physics, AHEPA University Hospital, Aristotle University Medical School, Thessaloniki Greece
empapana@med.auth.gr

Received:
30 May 2017
Accepted revised:
28 July 2017

Abstract

Objectives: In cardiac I-123 (^{123}I) imaging downscatter from high energy emissions degrades the image and introduces distortion of semi-quantitative analysis when using a low energy collimator. The effect of a triple energy window (TEW) scatter correction technique, using windows immediately above and below the principal window centered on 159keV, was examined. **Materials and Methods:** A hemispherical cardiac phantom was inserted into a cylindrical phantom and both were filled with radioactive ^{123}I water solutions. Phantoms were submitted to planar and tomographic scintigraphy under various acquisition and processing conditions, including the use of medium energy (ME) and low energy (LE) collimation. **Results:** In planar imaging, there was a distance dependent count loss with the LEHR collimator which was partly restored with TEW correction. There was minimal dependence of count rate with distance in using ME collimation. Conversely, the heart to background (H/B) ratio increased with increasing distance with the LEHR collimator, but in applying the TEW correction that ratio paralleled the minimally affected values obtained with the ME collimation. In tomographic imaging the acquired H/B ratio was lower with LE collimation alone, in comparison to the ME collimator, but it was raised significantly when applying the TEW scatter correction. Quantitative measurements also depended on the background method and the reconstruction algorithm applied. **Conclusion:** In cardiac ^{123}I imaging with a LE collimator the use of TEW scatter correction provides a semi-quantitative assessment comparable to that attained with ME collimation and may moderate inter-institutional inconsistencies.

Hell J Nucl Med 2017; 20(2): 154-159 *Published online: 8 August 2017*

Introduction

Iodine-123 (^{123}I) is a radionuclide used in several examinations in nuclear medicine including: (a) ^{123}I metaiodobenzylguanidine (MIBG) scintigraphy for the evaluation of sympathetic cardiac function [1]; (b) uptake measurements in thyroid scintigraphy [2]; (c) quantitative analysis of dopaminergic receptors with [^{123}I]-CIT [3] and (d) beta-methyl-p-(^{123}I)-iodophenyl pentadecanoic acid (BMIPP) for the assessment of fatty acid metabolism of the myocardium [4].

In these examinations images are acquired by collecting photons within an energy window centered at the 159keV photopeak of ^{123}I. However, this isotope emits also high energy gamma rays, with a prominent (1.4% abundance) 529keV photopeak, which give rise to downscatter and penetration in the septa of the collimator, degrading the image quality of the unscattered 159keV gamma rays. This deterioration can have a significant impact on quantitative accuracy and on clinical assessment in both planar and tomographic imaging [5].

Regarding cardiac ^{123}I MIBG scintigraphy, the heart-to-mediastinum (H/M) ratio has proven to be very useful and with relatively low intra-observer and inter-observer variability [6-8]. However, considerable overlap in the values of H/M ratio for health and disease have been reported, whereas the lack of a worldwide accepted standardization in acquisition and processing may result in inconsistencies between institutions [9-12]. Certain authors propose the use of a medium energy collimator for ^{123}I imaging to moderate the effects caused by the high energy emissions [5, 13-14]. Although not advocated by official recommendations, however, the use of a low energy collimator may offer advantages in both resolution and sensitivity. Indeed, other investigators have suggested different ways to correct for the degrading effects of downscatter, such as multiwindow acquisition modes [15, 16]. Nonetheless, previous work acknowledged issues and provided not always concurring solutions for those problems, whereas data for single-photon

emission tomography (SPET) are limited. Thus much room is left for assessing the effectiveness of various amendments in attaining quantitative accuracy [14-17].

In this phantom study, we focused on the multiple-window method with a low energy high resolution collimator (LEHR) as a practical approach that can be applied in any institute, and is not influenced by camera vendors and the specifications of collimators. We hypothesized that this approach would be equivalent to acquisitions with a medium energy general purpose collimator (MEGP) in restoring distortions in the quantification of cardiac ^{123}I MIBG scintigraphy, both in planar and tomographic imaging. In this respect, various factors that would influence quantitative analysis were investigated.

Materials and Methods

Phantoms

A hemispherical cardiac phantom (Veenstra PS-CI, Veenstra Instruments, Joure, The Netherlands) with both a circular base diameter and a height of 8cm, was filled with a radioactive solution of ^{123}I (6.0MBq in 240mL of water) and it was placed in the centre of a cylindrical tomographic phantom (Veenstra PS-101, Veenstra Instruments, Joure, The Netherands) with a circular base diameter of 20cm and a height of 30cm, from which the tomographic inserts were removed (Figure 1a). This setting resembles human ^{123}I cardiac MIBG studies. The tank was uniformly filled with two different ^{123}I radioactive solutions (initially 15.3MBq and subsequently 23.4MBq in 7100mL of water). The activities inserted into the cardiac phantom and the cylindrical tank were properly chosen in order to provide two different cardiac to background radioactive concentration ratios of approximately 12:1 and of 8:1. A series of preparatory measurements with planar imaging in our institution had determined that these concentrations provided heart to background ratios in the range of 1.9-2.7. Within this range, cut-off values of normality are commonly set in cardiac MIBG imaging [6, 18, 19].

After completion of acquisitions, 1mL aliquots were withdrawn from both the cardiac and the background solutions and were measured in a well type gamma counter (Cobra II, Packard Instrument Company, Meriden, CT) in order to verify the exact radioactive concentration ratios.

Acquisition and processing

Acquisitions were performed with a single-headed ADAC Genesys SPET gamma camera (ADAC Labs. Milpitas, CA), equipped with a 3/8" sodium iodide scintillation crystal and interfaced with a Pegasys processing workstation. The axis of the cyindrical phantom was parallel to the axis of rotation of the camera head. Two different collimators, as supplied by the gamma camera manufacturer, were used: a LEHR and a MEGP. Both collimators were of the hexagonal parallel-hole type and their specifications are listed in Table 1.

For both radioactivity concentration ratios, planar images were acquired with both collimators at three different phantom-collimator distances, namely 2, 10 and 20cm. All images were acquired on a 256x256 matrix, with a 1.46 zoom (pixel size: 1.6mm) and an acquisition time of 300sec.

Separate tomographic acquisitions were performed over a 360° circular orbit, with a radius of rotation of 23cm, using a 64x64 matrix, a 1.85 zoom factor (pixel size: 5.1mm), in 120 projections and an acquisition duration of 15sec/projection. Projection data were reconstructed using both a filtered back-projection (FBP) algorithm and an iterative reconstruction algorithm with 10 iterations, as provided by the gamma camera software (AutoSPET plus). A Butterworth low pass filter function with a cut-off frequency of 0.30 and an order of 10 were used in prefiltering for back-projection and postfiltering for iterative reconstructions. The selection of the filtering parameters was based on the results of a preparatory study performed in our department prior to the present study.

Table1. *LEHR and MEGP collimator specifications.*

Collimator	Hole size (mm)	Hole length (mm)	Septal thickness (mm)	Number of holes
LEHR	1.40	32.8	0.152	89600
MEGP	2.95	48.0	1.143	12900

Scatter and attenuation correction

MEGP images were acquired using only the 159keV±10% photopeak window, and hence no scatter correction was applied. LEHR images were acquired in three separate energy windows, a central 159keV±10% photopeak window (144keV-174keV, window width 31keV, $Image_{cen}$), a 138± 8% low energy scatter window (133keV-143keV, window width 11keV, $Image_{low}$) and a 180±6% high energy scatter window (175keV-185keV, window width 11keV, $Image_{high}$). The 159 keV±10% photopeak images, without any further processing, served as scatter uncorrected LEHR images (LEHR-No-SC). The images acquired at the scatter windows were added and then scaled by a factor of 1.41 ([31/(2x11)]x[$Image_{low}$ + $Image_{high}$]) in order to balance for the different energy window widths. Subsequently, they were subtracted from the photopeak images to produce the Triple Energy Window scatter corrected LEHR images (LEHR-TEW). In tomographic imaging the TEW correction was applied to the projection data prior to the reconstruction. Chang's attenuation correction was applied also using an attenuation coefficient of $\mu=0.12cm^{-1}$ for ^{123}I.

Processing and semi-quantitative analysis

In planar images Regions of Interest (ROI) of the heart (H) and the background (B) were drawn in order to calculate the H/B ratios (Figure 1b). A semi-elliptical ROI was drawn to fit the heart phantom, including the heart cavity. Two different background ROI were manually drawn: the first was a rectan-

gular ROI placed at the lower end of each image (B1), and the second was an irregular ROI surrounding the Heart ROI (B2). In addition, three ROI were drawn at the periphery of the planar images, to the left, to the right and above the cylindrical phantom, and their mean count density was calculated (OutROI-Figure 1c).

In tomographic studies Volumes of Interest (VOI) of the heart and the background were used to calculate the H/B ratios. A Region of Interest (ROI) was drawn to encompass the entire heart using a simple segmentation algorithm: On each reconstructed slice, all pixels with a count density above 50% of the global image maximum were included in the heart ROI. A rectangular ROI was drawn at the lower end of each reconstructed slice and a second doughnut-shaped ROI was drawn on each reconstructed slice surrounding the heart (Figure 1d). The sum of these ROI in all reconstructed slices produced the heart and background (B1 and B2) VOI. The H/B ratios were calculated from the mean counts per voxel in the VOI of the heart and the background before and after LEHR-TEW correction.

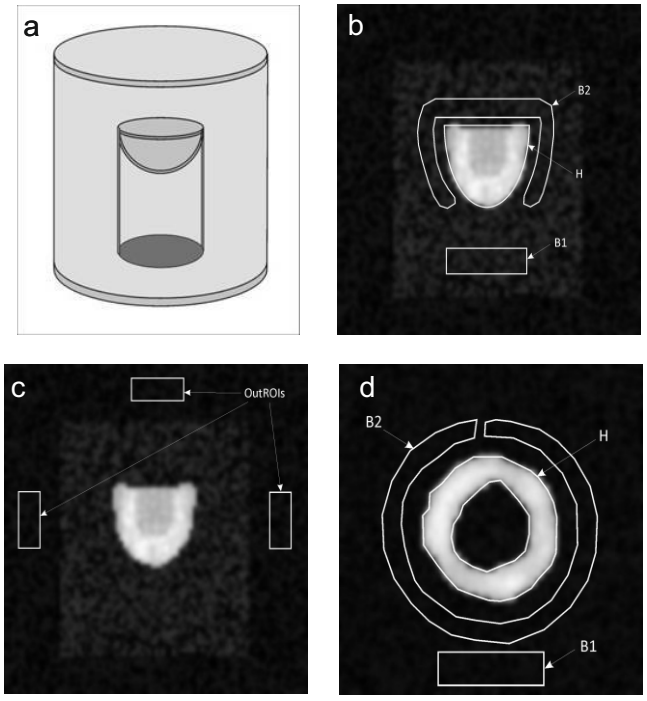

Figure 1. (a) Sketch of the cardiac phantom inside the cylindrical phantom. (b) Planar image with heart and background ROI shown. (c) Planar image with OutROI shown. (d) Typical slice of a SPET image with heart and background ROI shown.

Statistical analysis

Statistical analysis was performed with the SPSS v.17 software (SPSS Inc., Chicago). Normal distribution of the semi-quantitative parameters was checked with Kolmogorov-Smirnov tests. Paired samples t-tests and Wilcoxon signed rank tests were appropriately used to compare the calculated H/B ratios between different collimators and applied corrections. Statistical significance was accepted for $P<0.05$.

Results

Well-counter measurements showed that the actual H/B radioactivity ratios were 11.5:1 and 7.6:1. The results described below were similar for both radioactivity concentration ratios.

Planar imaging

In planar MEGP images, the count density in the OutROI was very low and practically independent on the phantom-to-collimator distance for both radioactivity concentration ratios (Figure 2). However, in the planar LEHR-NoSC images the OutROI count densities dropped considerably as the phantom-to-collimator distance increased (by 37% from 2cm to 20cm). This distance-dependent count density reduction was less prominent when the TEW correction was applied (a 26% decrease from 2cm το 20cm).

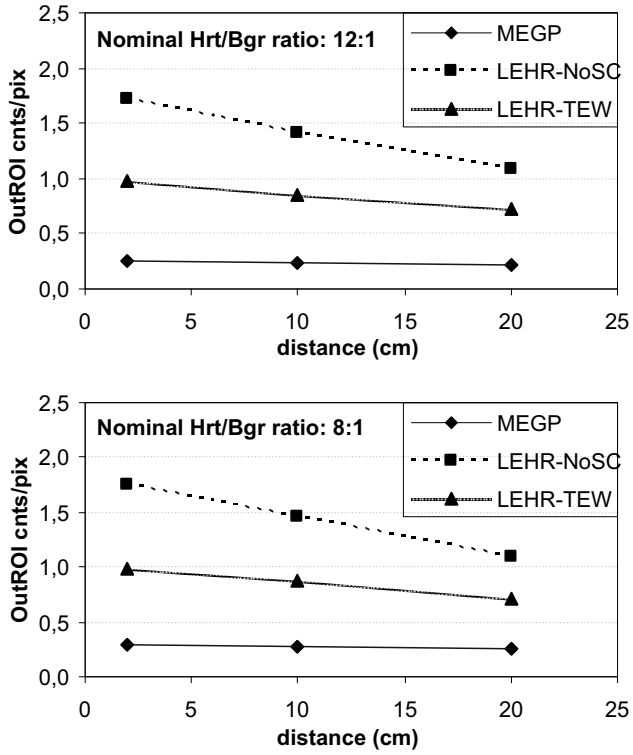

Figure 2. Variation of OutROI count density with phantom-to-collimator distance for the three acquisition-processing combinations (MEGP, LEHR-NoSC and LEHR-TEW).

Both H/B1 and H/B2 showed a small drop with increasing phantom-to-collimator distance for both radioactivity concentration ratios (5% drop from 2cm to 20cm on average) with the MEGP collimator (Figure 3). Conversely, those ratios raised with increasing distance in the LEHR-NoSC images (on average by more than 8%). By applying the LEHR-TEW correction the H/B ratios were closer to the values obtained with the MEGP collimator (on average a rise of 1%) (Figure 3).

Tomographic imaging

In tomographic imaging the calculated H/B ratios in general were approximately 50% lower than the nominal ones. Calculated H/B ratios with the MEGP collimator were higher

than those with the LEHR-NoSC (P=0.001), with either background or reconstruction algorithm used and for both radioactivity concentration ratios. The application of the TEW correction, increased dramatically the H/B ratios compared to the uncorrected ones (P<0.001). The LEHR-TEW corrected ratios also were significantly higher (P<0.001) in comparison to the MEGP measurements (Figure 4).

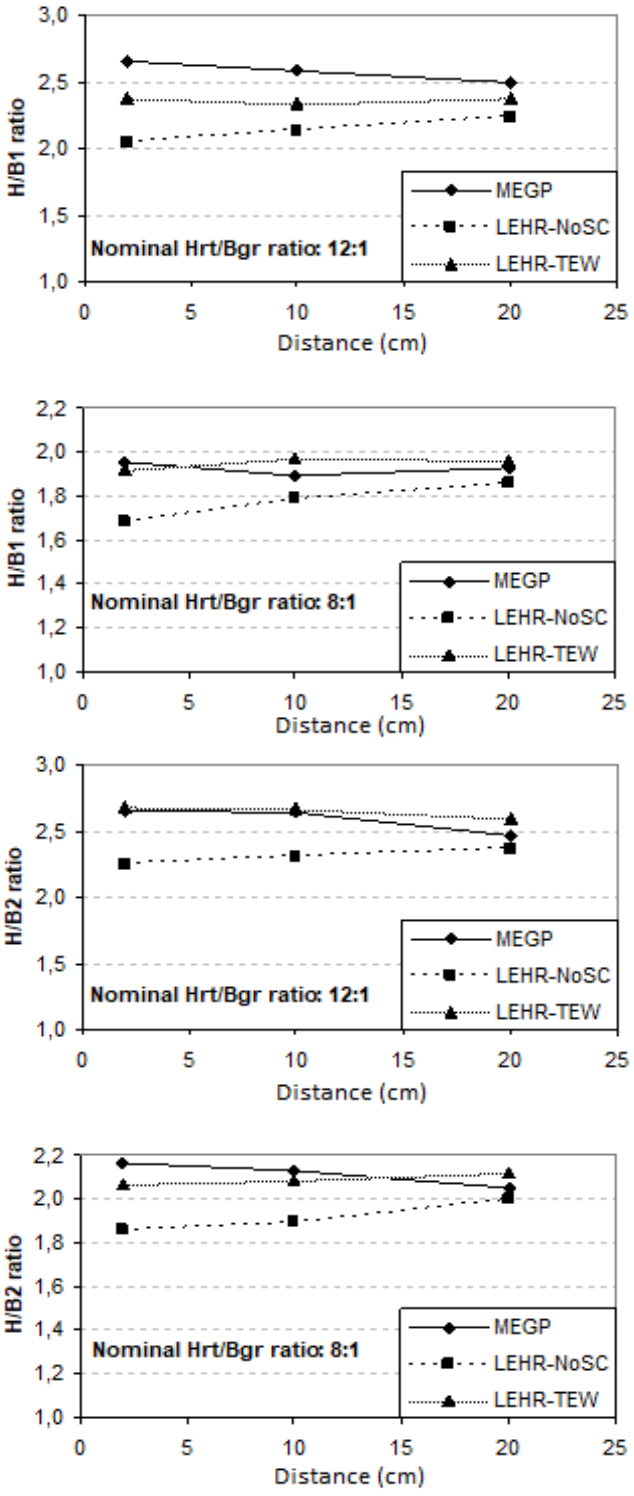

Figure 3. Variation of planar H/B ratios as a function of phantom-to-collimator distance for the three acquisition-processing combinations (MEGP, LEHR-NoSC and LEHR-TEW) and the two background ROI (B1, B2) used. At small distances, MEGP produced the highest ratios, followed by LEHR-TEW.

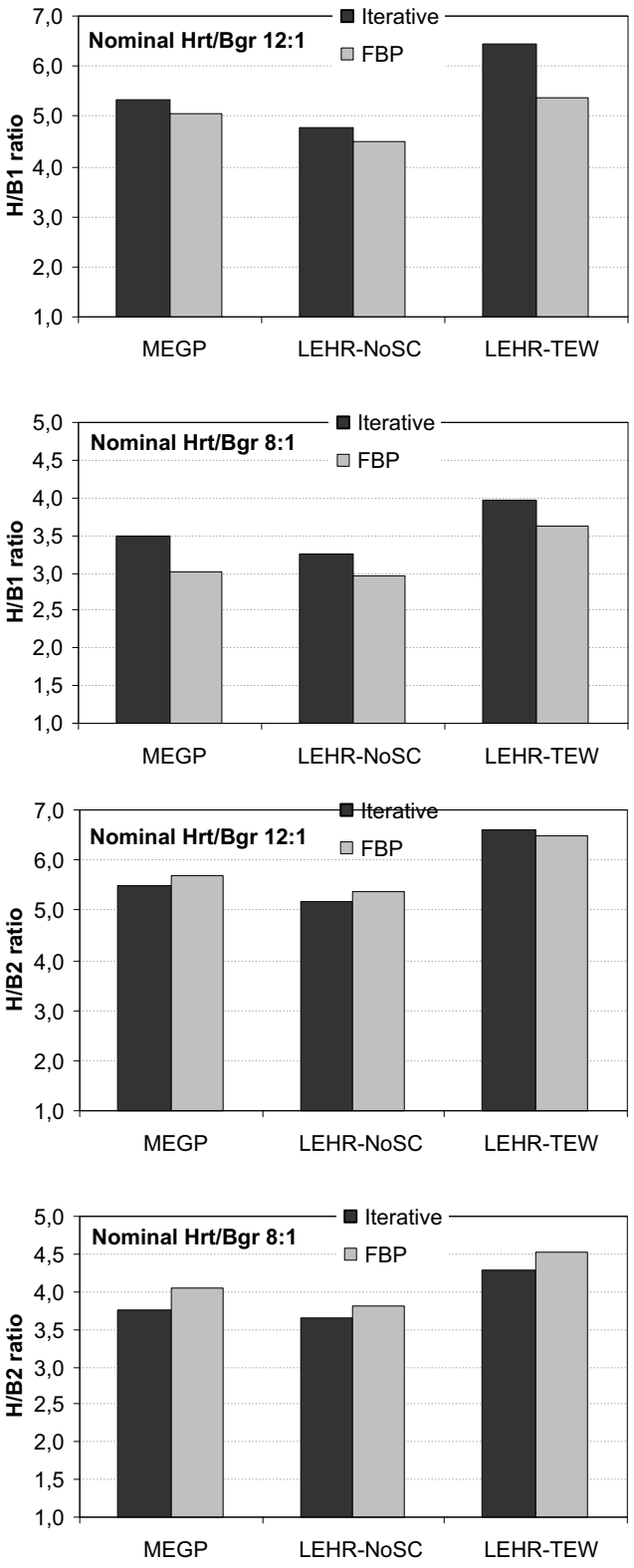

Figure 4. SPET heart/background ratios (H/B1 and H/B2) for the three acquisition-processing combinations (MEGP, LEHR-NoSC and LEHR-TEW) as a function of the method of reconstruction (iterative or FBP). The LEHR-TEW combination always produced higher ratios than MEGP (P=0.001), which in turn always produced higher ratios than LEHR-NoSC (P<0.001).

Regarding the background ROI used, H/B2 ratios were significantly higher than H/B1, irrespective of the reconstruction

method used (P=0.004), the differences being more pronounced for the FBP, for both radioactivity concentration ratios. Concerning the reconstruction algorithm used, H/B1 calculated from the iteratively reconstructed slices tended to be higher than that calculated from the FBP reconstructed data, but statistical significance was not reached (P=0.086). On the other hand, H/B2 calculated from the FBP reconstruction was significantly higher (P=0.033) than that calculated from the iterative reconstruction (Figure 4).

Discussion

In routine clinical imaging with radionuclides the choice of collimator involves balancing spatial resolution against sensitivity. This is particularly important when imaging with ^{123}I, where there is a significant component of scatter from higher energy photons. In a phantom setting that resembles the conditions under which clinical ^{123}I cardiac imaging is performed, this study complements and reinforces previous work by demonstrating that the quantitative results are affected significantly by a number of variables, namely the type of collimator, the collimator-to-source distance in planar imaging and the selection of background and the processing algorithm in tomographic imaging.

With commonly used isotopes in nuclear medicine the geometrical sensitivity of the parallel-hole collimators does not depend on phantom-to-collimator distance. Therefore, measured counts and indices based on radioactivity ratios remain constant with changing distance, irrespective of the collimator choice. Conversely, when imaging ^{123}I with LEHR or LEGP collimators, a significant amount of high energy photons (>400keV) penetrates the septa, with or without interaction with the lead. These scattered and not scattered photons may then be detected in the 159keV photopeak window and, since they are not perpendicular to crystal surface, they may blur the image and also distort count measurements. These distortions may be mitigated by correcting for downscatter [15, 16].

The MEGP collimator has a septal thickness several fold the thickness of a LEGP or LEHR collimator. A 529keV photon, which undergoes scattering repeatedly to be reduced to an energy level of 159keV, would rather not escape an ME collimator, particularly as in lower energies a photon is more likely to undergo photoelectric absorption than Compton scattering. Thus, unlike a LEHR collimator, MEGP collimation substantially reduces the contribution of downscatter to the image. However, the latter generally provides not only reduced sensitivity but also relatively low spatial resolution, which may interfere with image details and accurate estimation of activity in small regions. The TEW downscatter correction applied in this and previous studies corrects for the contribution of downscatter to the image in the LEHR collimator, while improved spatial resolution is maintained.

The decrease in count rate measurements as an ^{123}I source is moved away from the surface of a LEHR collimator, which is shown in this study (Figure 2), has been reported previously [5, 16] and it has been proposed that downscatter correction could compensate for this [15, 16]. The effectiveness of the TEW method in correcting for the septal penetration of the high energy ^{123}I photons can be estimated by measuring the count density in areas of the image outside the cylindrical phantom, where no counts are normally expected. The greater the angle subtended between the collimator and the source, the greater the proportion of lead within the radiating sphere of the source, namely the amount of scattering material. As the source is moved away from the collimator the subtended angle is reduced and hence the volume of scattering material, whereas the effective path of an incident photon in the septa is increased and with it the attenuation in the scattering material. Hence, at longer source-to-collimator distances fewer high energy photons undergo downscatter and fewer are incident on the crystal into the imaging window centered on 159keV.

The variation in count rate with distance in ^{123}I imaging would lead to errors in the H/M ratio in cardiac ^{123}I MIBG imaging. Indeed, in our experimental setting the H/B ratio decreased at shorter phantom-to-collimator distances in the LEHR-NoSC images, for both backgrounds used (B1 and B2). Probably, this is the result of comparatively increased scatter measurements from the high energy photons in areas surrounding the phantom over shorter source-to-collimator distances. In other words, the penetration component decreases significantly with increasing phantom-to-collimator distance and vice versa and it affects mostly those areas in the image that are closer to higher activity regions, namely, the background ROI counts are affected more compared to the heart ROI counts. For the MEGP collimator, however, the H/B ratios were minimally affected by the phantom-to-collimator distance, as a result of a significantly depressed septal penetration. In the corrected LEHR-TEW images, penetration counts were taken into account in all ROI and measured ratios were restored to levels closer to those of the MEGP collimator (Figure 3).

The normal range of H/M ratio in MIBG varied significantly among many institutions [6, 18, 19]. Apparently, to a certain extent this may be due to the type of collimator used and its particular specifications which may differ between manufacturers. This variability may unfavorably affect meta-analyses and comparisons between published series. This study demonstrates that the use of TEW with a LEHR collimator provides results closer to those determined with a MEGP collimator and thus it may blunt considerably the inconsistencies between institutions and recommendations between authors [20, 21].

In agreement with other investigators, both MEGP and LEHR provided measured ratios considerably less than the nominal ones in the experimental setting, particularly in planar scintigraphy, in which the superimposed counts from other anatomical structures cause low ratios between myocardium and reference organs [22]. The improved image contrast in tomographic imaging would be expected to provide measured ratios even closer to the actual radioactivity concentration ratios. In this regard, since SPET would be used to better evaluate regional impairment of cardiac sympathetic function a LEHR collimator with improved spatial resolution would be preferable. However, the quantitative distortions

present with ^{123}I and a LEHR collimator in planar imaging would propagate in SPET reconstructions, as shown previously [20]. Moreover, the heart is not equidistant to the collimator over the orbit, whereas the radius of rotation cannot be set less than a certain length.

In this work, in tomographic imaging the H/B ratios were closer to the actual concentration ratios, as compared to planar acquisition, yet quite distant (Figure 4). These findings parallel previous data [7]. Moreover, the results depended significantly on the background method and also the reconstruction algorithm employed. Interestingly, TEW correction in acquisitions with a LEHR collimator outperformed MEGP in attaining H/B values closer to the nominal ratios. In a previous work a special LEHR collimator with less septal penetration than a simple LEHR collimator provided higher quantitative accuracy than MEGP collimation in SPET imaging [23]. Finally, in our study there was no linear proportionality between radioactivity concentrations and measured count ratios in both planar and tomographic acquisitions as significant increments of the former corresponded to small changes in the latter. An earlier work has also shown non-proportionality between measured and theoretical count rate ratios in ^{123}I SPET imaging and also a superiority of OSEM over FBP reconstruction in image contrast [17].

Limitations

The experimental setting used resembles, but is not identical to clinical conditions of cardiac ^{123}I MIBG imaging, which may be influenced by additional factors, such as the radioactivity accumulation in neighbouring organs. Moreover, manually drawn ROI may affect the reproducibility of measurements, whereas a source-to-collimator distance of 20cm is unrealistic in clinical planar acquisitions. Nevertheless, the principles underlying image degradation from high energy emissions and restoration of quantitative measurements with the TEW scatter correction method that were discussed in this study are also valid in clinical ^{123}I MIBG imaging.

In conclusion: In cardiac imaging with ^{123}I the use of a LEHR collimator offers a sensible compromise between sensitivity and spatial resolution. The influence of high-energy photons on semiquantitative analysis may be counterbalanced by a TEW scatter correction in both planar and tomographic imaging, providing results comparable to those of a MEGP collimator. Nevertheless, careful standardization of acquisition and processing variables is required to facilitate inter-institutional interchangeability of quantitative measurements in ^{123}I imaging.

Bibliography

1. Merlet P, Valette H, Dubois-Rande J et al. Prognostic value of cardiac metaiodobenzylguanidine imaging in patients with heart failure. *J Nucl Med* 1992; 33: 471-7.
2. Robeson WR, Ellwood JE, Castronuovo JJ, Margouleff D. A new method to measure thyroid uptake with a gamma camera without routine use of a standard source. *Clin Nucl Med* 2002; 27: 324-9.
3. Messa C, Volonte M, Fazio F et al. Differential distribution of striatal [^{123}I]-CIT in Parkinson's disease and progressive supranuclear palsy, evaluated with single-photon emission tomography. *Eur J Nucl Med* 1998; 25: 1270-6.
4. Yazaki Y, Isobe M, Takahashi W et al. Assessment of myocardial fatty acid metabolic abnormalities in patients with idiopathic dilated cardiomyopathy using ^{123}I BMIPP SPECT: correlation with clinicopathological findings and clinical course. *Heart* 1999; 81: 153-9.
5. Dobbeleir AA, Hambye ASE, Franken PR. Influence of high energy photons on the spectrum of iodine-123 with low and medium energy collimators: consequences for imaging with ^{123}I-labelled compounds in clinical practice. *Eur J Nucl Med* 1999; 26: 655-8.
6. Somsen GA, Verberne HJ, Fleury E, Righetti A. Normal values and within-subject variability of cardiac I-123 MIBG scintigraphy in healthy individuals: Implications for clinical studies. *J Nucl Cardiol* 2004; 11: 126-33.
7. Somsen GA, Borm JJJ, de Milliano PAR et al. Quantitation of myocardial iodine-123 MIBG uptake in SPET studies: a new approach using the left ventricular cavity and a blood sample as a reference. *Eur J Nucl Med* 1995; 22: 1149-54
8. Veltman CE, Boogers MJ, Meinardi JE et al. Reproducibility of planar ^{123}I-meta-iodobenzylguanidine (MIBG) myocardial scintigraphy in patients with heart failure. *Eur J Nucl Med Mol Imaging* 2012; 39: 1599-608.
9. Nagayama H, Hamamato M, Ueda M et al. Reliability of MIBG myocardial scintigraphy in the diagnosis of Parkinson's Disease. *J Neurol Neurosurg Psychiatry* 2005; 76: 249-51.
10. Yamashina S, Yamazaki J. Role of MIBG myocardial scintigraphy in the assessment of heart failure: the need to establish evidence. *Eur J Nucl Med Mol Imag* 2004; 31: 1353-5.
11. Motherwell DW, Petrie MC, Martin W, Cobbe SM. ^{123}I metaiodobenzylguanidine in chronic heart failure: is there a clinical use? *Nucl Med Commun* 2006; 27: 927-31.
12. Flotats A, Carrió I, Agostini D et al. Proposal for standardization of ^{123}I metaiodobenzylguanidine (MIBG) cardiac sympathetic imaging by the EANM Cardiovascular Committee and the European Council of Nuclear Cardiology. *Eur J Nucl Med Mol Imaging* 2010; 37: 1802-12.
13. Inoue Y, Suzuki A, Shirouzu I et al. Effect of collimator choice on quantitative assessment of cardiac iodine-123 MIBG uptake. *J Nucl Cardiol* 2003; 10: 623-32
14. Verbeme HJ, Feenstra C, de Jong WM et al. Influence of collimator choice and simulated clinical conditions on ^{123}I-MIBG heart/mediastinum ratios: a phantom study. *Eur J Nucl Med Mol Imaging* 2005; 32: 1100-7.
15. Kobayashi H, Momose M, Kanaya S et al. Scatter correction by two-window method standardizes cardiac I-123 MIBG uptake in various gamma camera systems. *Ann Nucl Med* 2003; 17: 309-13.
16. Small AD, Prosser J, Motherwell DW et al. Downscatter correction and choice of collimator in ^{123}I imaging. *Phys Med Biol* 2006; 51: N307-N11.
17. Yang YW, Chen JC, Chang et al. Evaluation of collimator choice and scatter correction on ^{123}I SPECT images. *Nuclear Instruments and Methods in Physics Research* 2008; A 584: 20.
18. Morozumi T, Kusuoka H, Fukuchi K et al. Myocardial iodine-123-metaiodobenzylguanidine images and autonomic nerve activity in normal subjects. *J Nucl Med* 1997; 38: 49-52.
19. Merlet P, Benvenuti C, Moyse D et al. Prognostic value of MIBG imaging in idiopathic dilated cardiomyopathy. *J Nucl Med* 1999; 40: 917-23.
20. Macey D J, DeNardo GL, DeNardo S, Hines HH. Comparison of low- and medium-energy collimators for SPECT imaging with iodine-123-labelled antibodies. *J Nucl Med* 1986; 27: 1467-74.
21. Gilland DR, Jaszczak R J, Turkington TG et al. Volume and activity quantitation with iodine-123 SPECT. *J NuclMed* 1994; 35: 1707-13.
22. Nakajima K,Matsubara K, RT, Ishikawa T et al. Correction of iodine-123-labeled meta-iodobenzylguanidine uptake with multi-window methods for standardization of the heart-to-mediastinum ratio. *J Nucl Cardiol* 2007; 14: 843-51
23. Inoue Y, Shirouzu I, Machida T et al. Collimator choice in cardiac SPECT with I-123-labeled tracers. *J Nucl Cardiol* 2004; 11: 433-9.